Optimal Control Model for The Spread of Tungro Disease in Rice Plants by Controlling Using Pesticides

Rika Amelia, Nursanti Anggriani, Asep K. Supriatna, and Noor Istifadah

***Abstract*—Rice Tungro Bacilliform Virus (RTBV) and *Rice Tungro Spherical Virus* (RTSV) cause Tungro virus disease. Although the two viruses have different characteristics, the green leafhopper, which only sucks on RTSV-infected plants, can catch and transmit RTSV. However, green leafhoppers, which only feed on RTBV-infected rice plants, cannot notice RTBV, and no transmission occurs. Meanwhile, when a green leafhopper sucks a plant infected with RTSV and then sucks a plant infected with RTBV, the green leafhopper can transmit both viruses. Pesticides can control the spread of tungro, but excessive use can cause losses to farmers. Furthermore, control theory and dynamic analysis are used to analyze the spread of the disease and determine the best use of pesticides to get the optimal solution. The results show that using specifications can reduce the intensity of the infected population.**

***Index Terms*—Tungro disease, mathematical modeling, Characteristics of the Virus, dynamical analysis, optimal control.**

I. Introduction

THE rice plant (*Oryza sativa* L.) is a plant that has an essential role in the Indonesian economy. Apart from enabling poverty alleviation, this can also increase income and create jobs. However, farmers often experience problems cultivating rice, such as being attacked by pests and diseases [1-3].

Farmers often face diseases while growing rice, including the tungro virus. It is caused by RTSV and RTBV, transmitted by the green leafhopper (*Nephotettix virescens*) in a semipersistent manner without a latent period. The two viruses have distinct characteristics, and the leafhopper can spread both simultaneously. Furthermore, when the leafhopper feeds on plants infected with RTSV, it can transmit the virus but cannot transmit RTBV when feeding on RTBV-infected plants. However, feeding on RTSV-infected and RTBV-infected plants can transmit both viruses [4-7].

Infected vectors play an essential role in the spread of tungro virus disease. Therefore, studying population dynamics in the spread of Tungro Virus Disease (TVD) by considering virus characteristics is very important. Further analysis can be obtained by constructing a mathematical model [8]. The spread of TVD can be controlled through pesticides, but excessive pesticide use can negatively impact farmers. Therefore, an optimal control model must be developed to maintain and optimize pesticide use. Many mathematical models of the spread of plant diseases have been created by previous researchers, such as mathematical models of yellow disease in chili plants [9-11], mathematical models considering control using fungicides [12-14], mathematical models considering curative factors, roguing, replanting, and preventive [15-21], and mathematical models of TVD [22-28].

Based on previous models, only some researchers are still discussing mathematical models for spreading TVD. This can be seen in Figure 1, which shows the results of a literature search using the keywords used by Amelia [28] (see Figure 1).

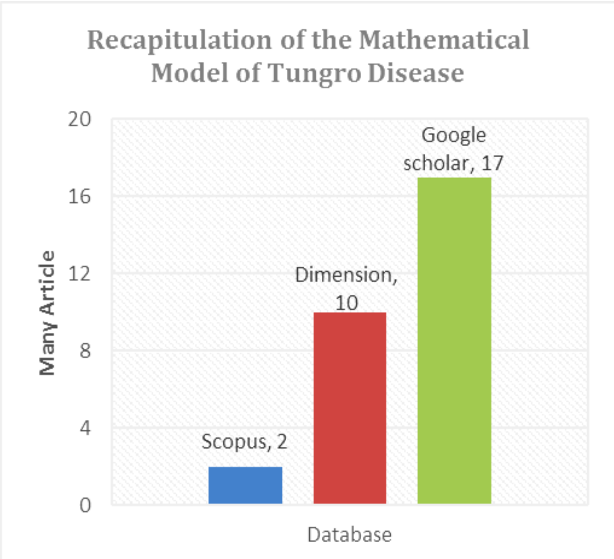

Fig. 1. The search results diagram on the Scopus, Dimension, and Google Scholar databases.

Only seven articles addressed the spread of the tungro virus disease in rice plants. In one study, Anggriani [18] reported the impact of insecticide usage on tungro disease

Manuscript received January 30, 2023; revised April 12, 2024.

This research is funded by Universitas Padjadjaran with contract number: 2064/UN6.3.1/PT.00/2022.

R. Amelia is a postgraduate student at the Department of Mathematics, Faculty of Mathematics and Natural Science, Universitas Padjadjaran, Bandung, Indonesia. E-mail: rika17003@mail.unpad.ac.id.

N. Anggriani is an associate professor at the Department of Mathematics, Faculty of Mathematics and Natural Science, Universitas Padjadjaran, Bandung, Indonesia. E-mail: nursanti.anggriani@unpad.ac.id

A. K. Supriatna is a professor at the Department of Mathematics, Faculty of Mathematics and Natural Science, Universitas Padjadjaran, Bandung, Indonesia. E-mail: a.k.supriatna@unpad.ac.id

N. Istifadah is an associate professor at Department of Plant Pathology, Faculty of Agriculture, Universitas Padjadjaran, Bandung, Indonesia. E-mail: n.istifadah@unpad.ac.id

vectors, while Suryaningrat [23] expanded the model to include biological factors and optimize control. Furthermore, the model was improved in 2022 with a spatiotemporal model [24]. Maryati [25] created a mathematical model that focuses on the growth phases of rice plants, dividing them into vegetative and generative phases.

Blas considered the characteristics of the virus in the constructed mathematical model of the spread of TVD [26] and the roguing factor in the model [27]. Research that researchers had previously carried out was analyzed before developing the mathematical model, which was then proven by mapping the seven articles in Figure 2 using *VOSviewer.*

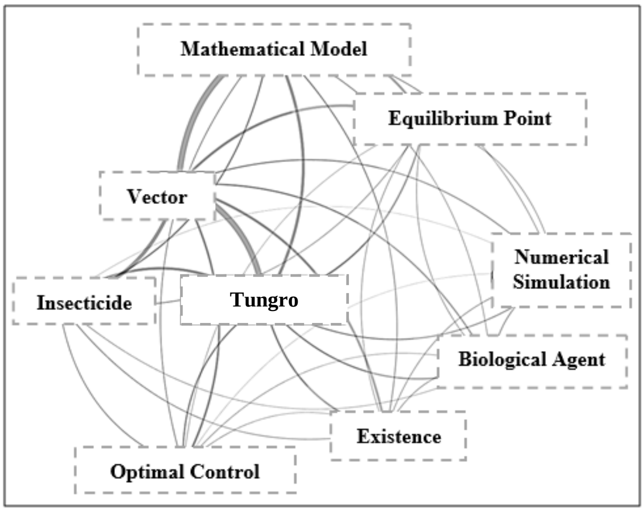

Fig. 2. Mapping results of seven articles discussing the model of the spread of TVD.

Figure 2 shows no nodes representing virus characteristics, no lines connecting the dynamic analysis (represented by the solution nodes of the equilibrium point and existence), and optimal control with characteristic virus nodes. This was also explained by Amelia [28] in her research, which stated that there had been no research discussing the analysis of mathematical models of the spread of TVD by considering the dynamic characteristics of the virus and determining its optimal control. Therefore, this research is intended to dynamically and numerically analyze Blas's mathematical model and create an optimal control model to determine the best pesticide dose. Thus, dynamic analysis is considered very important in studying the dynamic behavior of the model, while numerical simulations are carried out to confirm the analysis results.

II. Mathematical Model

This research will discuss the 2016 Blas mathematical model [26], using descriptions of parameters and variables and several parameter values used by Blas [26-27].

$$\frac{dP_0}{dt} = r(K - N_P) - \frac{\alpha P_0 V_3}{N_P} - \frac{\gamma P_0 V_3}{N_P} - \frac{\tau P_0 V_3}{N_P} - \frac{\beta P_0 V_1}{N_P} - \frac{\sigma P_0 V_2}{N_P} - q_0 P_0 \quad (1)$$

$$\frac{dP_1}{dt} = \frac{\beta P_0 V_1}{N_P} + \frac{\gamma P_0 V_3}{N_P} - \frac{\lambda P_1 V_3}{N_P} - q_1 P_1 \quad (2)$$

$$\frac{dP_2}{dt} = \frac{\tau P_0 V_3}{N_P} + \frac{\sigma P_0 V_2}{N_P} - \frac{\delta P_2 V_3}{N_P} - q_2 P_2 \quad (3)$$

$$\frac{dP_3}{dt} = \frac{\alpha P_0 V_3}{N_P} + \frac{\lambda P_1 V_3}{N_P} + \frac{\delta P_2 V_3}{N_P} - q_3 P_3 \quad (4)$$

$$\frac{dV_0}{dt} = BN_V\left(1 - \frac{N_V}{V}\right) - \frac{aP_3 V_0}{N_P} - \frac{bP_1 V_0}{N_P} + fV_2 - \mu V_0 \quad (5)$$

$$\frac{dV_1}{dt} = \frac{bP_1 V_0}{N_P} - \frac{gP_2 V_1}{N_P} - \mu V_1 \quad (6)$$

$$\frac{dV_2}{dt} = cV_3 - fV_2 - \mu V_2 \quad (7)$$

$$\frac{dV_3}{dt} = \frac{aP_3 V_0}{N_P} + \frac{gP_2 V_1}{N_P} - cV_3 - \mu V_3 \quad (8)$$

III. Dynamical Analysis

A. Positivity

Positivity is proven by stating the lemma below.

Lemma 1: If the initial value: $P_0(0) > 0, P_1(0) > 0, P_2(0) > 0, P_3(0) > 0, V_0(0) > 0, V_1(0) > 0,$ $V_2(0) > 0,$ and $V_3(0) > 0,$ solution of system $(1-8)$ is positive for all $t \in [0, t_1).$

Proof: Assumes that

$$\Omega(t) = \min\{P_0, P_1, P_2, P_3, V_0, V_1, V_2, V_3\}, \forall t > 0.$$

Obviously, $\Omega(0) > 0.$

Assume that there is $t_1 > 0.$

So that $\Omega(t_1) = 0$ and $\Omega(t) > 0,$ for all $t \in [0, t_1).$

If $\Omega(t_1) = P_0(t_1),$ then $P_0(t) > 0, P_1(t) > 0, P_2(t) > 0, P_3(t) > 0,$ $V_0(t) > 0, V_1(t) > 0, V_2(t) > 0, V_3(t) > 0,$ for all $t \in [0, t_1).$

From the model equation (1), we can obtain

$$\frac{dP_0}{dt} = r(K - N_P) - \frac{\alpha P_0 V_3}{N_P} - \frac{\gamma P_0 V_3}{N_P} - \frac{\tau P_0 V_3}{N_P} - \frac{\beta P_0 V_1}{N_P} - \frac{\sigma P_0 V_2}{N_P} - q_0 P_0$$

$$\frac{dP_0}{dt} = -\left(\frac{\alpha V_3}{N_P} - \frac{\gamma V_3}{N_P} - \frac{\tau_0 V_3}{N_P} - \frac{\beta V_1}{N_P} - \frac{\sigma V_2}{N_P} - q_0\right) P_0$$

$$\frac{dP_0}{P_0} = -\left(\frac{\alpha V_3}{N_P} - \frac{\gamma V_3}{N_P} - \frac{\tau_0 V_3}{N_P} - \frac{\beta V_1}{N_P} - \frac{\sigma V_2}{N_P} - q_0\right) dt$$

$$\int \frac{dP_0}{P_0} = \int -\left(\frac{\alpha V_3}{N_P} - \frac{\gamma V_3}{N_P} - \frac{\tau_0 V_3}{N_P} - \frac{\beta V_1}{N_P} - \frac{\sigma V_2}{N_P} - q_0\right) dt$$

$$\int \frac{dP_0}{P_0} = -\int \left(\frac{\alpha V_3}{N_P} - \frac{\gamma V_3}{N_P} - \frac{\tau_0 V_3}{N_P} - \frac{\beta V_1}{N_P} - \frac{\sigma V_2}{N_P} - q_0\right) dt$$

$$\ln|P_0| = -\int \left(\frac{\alpha V_3}{N_P} - \frac{\gamma V_3}{N_P} - \frac{\tau_0 V_3}{N_P} - \frac{\beta V_1}{N_P} - \frac{\sigma V_2}{N_P} - q_0\right) dt$$

$$|P_0| = \exp\left(-\int \left(\frac{\alpha V_3}{N_P} - \frac{\gamma V_3}{N_P} - \frac{\tau_0 V_3}{N_P} - \frac{\beta V_1}{N_P} - \frac{\sigma V_2}{N_P} - q_0\right) dt\right)$$

$$P_0 = \exp\left(-\int \left(\frac{\alpha V_3}{N_P} - \frac{\gamma V_3}{N_P} - \frac{\tau_0 V_3}{N_P} - \frac{\beta V_1}{N_P} - \frac{\sigma V_2}{N_P} - q_0\right) dt\right) \geq 0.$$

In the same way it is obtained $P_0, P_1, P_2, P_3, V_0, V_1, V_2, V_3 \geq 0.$

B. Boundary

Lemma 2: All solutions of system (1)-(8) are bounded for all $t \in [0, t_0].$

Proof:

To simplify the analysis, eg

$$q_0 = q_1 = q_2 = q_3 = \mu = q, r(K - N_P) = \psi, \text{and } BN_V\left(1 - \frac{N_V}{V}\right) = \omega.$$

Since $P_0 + P_1 + P_2 + P_3 + V_0 + V_1 + V_2 + V_3 = N,$ so

$$\frac{dN}{dt} = \frac{dP_0}{dt} + \frac{dP_1}{dt} + \frac{dP_2}{dt} + \frac{dP_3}{dt} + \frac{dV_0}{dt} + \frac{dV_1}{dt} + \frac{dV_2}{dt} + \frac{dV_3}{dt}$$
$$= \psi + \omega - \mu N.$$

So, we get:

$$0 \le \lim_{t\to\infty} N(t) \le \frac{\psi + \omega}{\mu}.$$

C. Disease-Free Equilibrium Poit (DFEP)

Make the infected compartment equal to zero to determine the DFEP obtained in equation (9).

$$E_0 = \{P_0, P_1, P_2, P_3, V_0, V_1, V_2, V_3\} = \left\{\frac{r(K - N_P}{q_0}, 0,0,0, BN_V\left(1 - \frac{N_V}{V}\right), 0,0,0\right\} \tag{9}$$

D. Basic Reproduction Number (BRN)

The BRN measures the average secondary infections produced by contagious individuals in a susceptible population, considering the virus transmission characteristics. The BRN is calculated using the next-generation matrix method since the spread of TVD does not have a latent population compartment. The process is based on Driessche's formulation [29]. So, obtained:

$$R_{01} = \zeta(\mathbf{FV}^{-1}) = \sqrt{\frac{BN_V\beta br(K - N_P)(V - N_V)}{Vq_0q_1\mu^2 N_P{}^2}},$$

$$R_{02} = \zeta(\mathbf{FV}^{-1}) = \sqrt{\frac{Ba\alpha r(K - N_P)N_V(V - N_V)}{q_0q_3V\mu N_P{}^2(c+\mu)}},$$

$$\text{and } R_0 = \max\{R_{01}, R_{02}\}.$$

F and **V** are the Jacobian matrices of matrix of movement rates in and out of the compartment calculated at the DFEP.

E. Stability analysis of DFEP

Theorem 1: The DFEP for the model of the spread of TVD considering the differences in the characteristics of the virus and roguing will be stable when $R_0 < 1$.

Proof: The stability of DFEP is obtained from the eigenvalues of substitution of DFEP into the Jacobian matrix model. The characteristic equation is obtained as follows

$$\frac{\left((\lambda+q_2)(\lambda+q_0)(\lambda+\mu)(\lambda+f+\mu)\left(a_0\lambda^4+a_1\lambda^3+a_2\lambda^2+a_3\lambda+a_4\right)\right)}{V^2\mu^2N_P{}^2q_0{}^2} = 0$$

So, $\lambda_1 = -q_2, \lambda_2 = -q_0, \lambda_3 = -\mu,$ and $\lambda_4 = -(f+\mu).$

A mathematical model of the spread of TVD considering the different characteristics of the virus will be asymptotically stable when $\lambda_i < 0$ for $i = 5,...,8.$ To prove that then it can be seen from the polynomial coefficients

$$a_0\lambda^4 + a_1\lambda^3 + a_2\lambda^2 + a_3\lambda + a_4 = 0$$

which was then tested using the Routh-Hurwitz criteria. Where:

$$a_0 = \left(V\mu N_P{}^2 q_0\right)^2 > 0$$

$$a_1 = \left(V\mu N_P{}^2 q_0\right)^2 (c + 2\mu + q_1 + q_3) > 0$$

$$a_2 = V\mu N_P{}^2 q_0 (q_0 V\left(\mu^2 + (2q_1 + 2q_3 + c)\mu + (q_3 + c)q_1 + q_3 c\right)\mu N_P{}^2 + BN_V r(a\alpha + b\beta)(K - N_P)(V - N_V)) > 0$$

$$a_3 = V\mu N_P{}^2 q_0 \left(\left(\left(BN_V r(a\alpha + b\beta) + b(q_3 + c)\beta + q_1\alpha a\right)(K - N_P)(V - N_V)\right) + \left((q_1 + q_3)\mu^2 + ((2q_3 + c)q_1 + q_3 c)\mu + q_1 q_3 c\right)\right) > 0$$

$$a_4 = \left(BN_V\beta br(K - N_P)(V - N_V) + Vq_0q_1\mu^2 N_P{}^2\right)\left(Ba\alpha r(K - N_P)N_V(V - N_V) + q_0q_3V\mu N_P{}^2(c+\mu)\right)$$

$$= \left(-R_{01}{}^2 + 1\right)\left(-R_{02}{}^2 + 1\right) > 0.$$

From the explanation above, it can be seen that $a_i > 0,$ for $i = 1,...,4$ if $R_{01}, R_{02} < 1.$ This means $\lambda_i < 0$ for $i = 5,...,8,$ if $R_{01}, R_{02} < 1.$ This proves that, a mathematical model of the spread of TVD taking into account the different characteristics of the virus will be asymptotically stable if $R_{01}, R_{02} < 1.$

IV. NUMERICAL SIMULATION

This numerical simulation supports the analytical results in the previous sub-chapter. The initial values and parameters used are shown in Table I.

TABLE I
VALUE OF PARAMETERS AND VARIABLES

Variable/ Parameter	Value	Unit	Citation
V_0	0	Vector	[27]
V_1	0	Vector	[27]
V_2	0	Vector	[27]
V_3	4000	Vector	[27]
P_0	0	Plant	[27]
P_1	0	Plant	[27]
P_2	0	Plant	[27]
P_3	20000	Plant	[27]
α	0.035	$\frac{\text{Plant}}{\text{Vector}\times\text{Day}}$	[26]
β	0.09	$\frac{\text{Plant}}{\text{Vector}\times\text{Day}}$	[26]
γ	0.01	$\frac{\text{Plant}}{\text{Vector}\times\text{Day}}$	[26]
σ	0.08	$\frac{\text{Plant}}{\text{Vector}\times\text{Day}}$	[26]
τ	0.06	$\frac{\text{Plant}}{\text{Vector}\times\text{Day}}$	[26]
a	0.996	$\frac{\text{Plant}}{\text{Vector}\times\text{Day}}$	[26]
b	0.996	$\frac{\text{Plant}}{\text{Vector}\times\text{Day}}$	[26]
c	0.5	$\frac{\text{Plant}}{\text{Vector}\times\text{Day}}$	[26]
f	0.33	$\frac{\text{Plant}}{\text{Vector}\times\text{Day}}$	[26]
g	0.996	$\frac{\text{Plant}}{\text{Vector}\times\text{Day}}$	[26]
q_0	0.008	$\frac{1}{\text{Day}}$	[26]
q_1	0.009	$\frac{1}{\text{Day}}$	[26]
q_2	0.0125	$\frac{1}{\text{Day}}$	[26]
q_3	0.0125	$\frac{1}{\text{Day}}$	[26]
r	0.001	$\frac{1}{\text{Day}}$	[26]
B	0.033	$\frac{1}{\text{Day}}$	[26]
V	100000	Vector	[26]

Variable/ Parameter	Value	Unit	Citation
K	30000	Plant	Assumption
δ	0.07	$\frac{\text{Plant}}{\text{Vector} \times \text{Day}}$	[26]
λ	0.03	$\frac{\text{Plant}}{\text{Vector} \times \text{Day}}$	[26]
μ	0.033	$\frac{\text{Plant}}{\text{Vector} \times \text{Day}}$	[26]

Using the values in Table I, a graph is obtained to study population dynamics numerically.

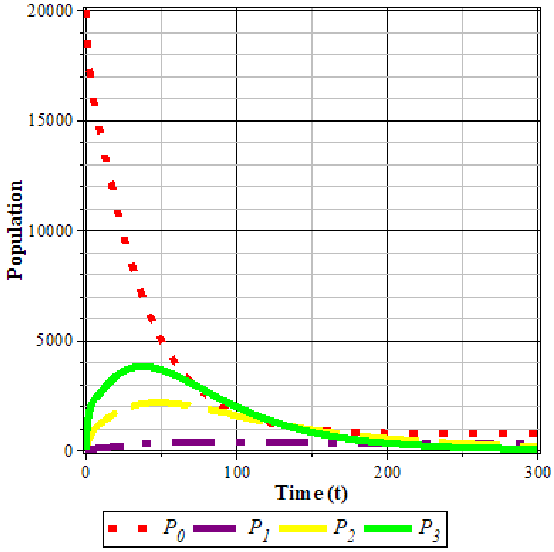

Fig. 3. Population dynamics of rice plants when $R_0 < 1$

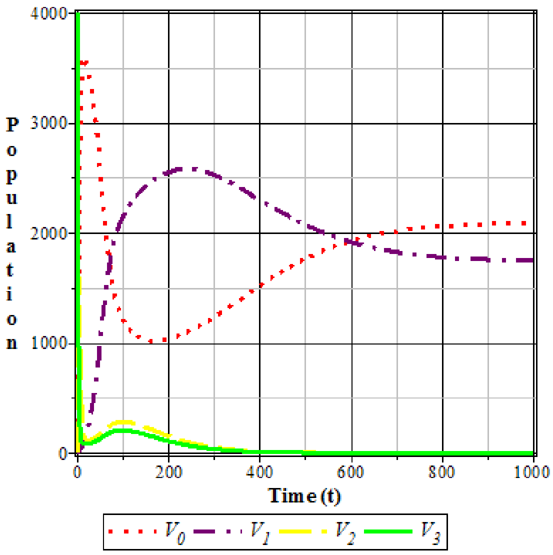

Fig. 4. Vector population dynamics when $R_0 < 1$.

Figure 3 shows the evolution of P_3 and P_2, as well as those that are susceptible. At the start of planting, P_3 increased, then declined until extinction after three months. P_1 also experienced an increase, followed by a drop until extinction after four months. In contrast, P_0 decreased initially, but this was due to a high number of infected plants, leading to a drastic decrease. Meanwhile, those P_1 showed an increase in the first three months, then a reduction for the next five, ultimately stabilizing at approximately 900 plants.

Figure 4 shows the population changes of V_3 and V_2. The population declined drastically in the first month and became extinct after the sixth. On the other hand, V_1 experienced an increase in population initially, followed by a decrease before extinction after the sixth month. V_0 increased in the first month, then a drastic reduction, before experiencing another increase after the sixth month. This is because some infected vector became susceptible through retention. Furthermore, V_1 experienced an increase in population at the start of the first month, followed by a decrease after the sixth.

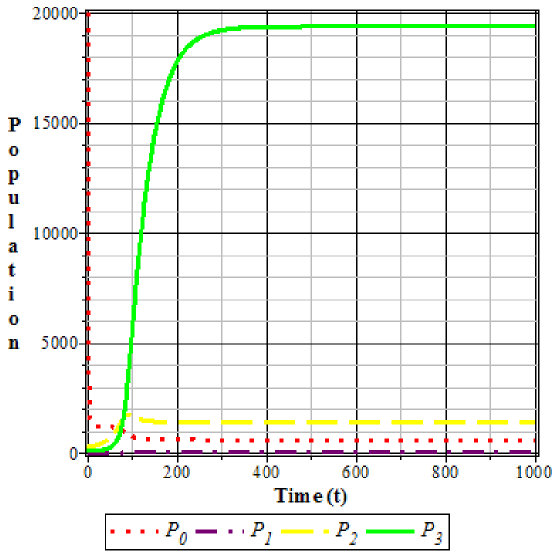

Fig. 5. Population dynamics of rice plants when $R_0 > 1$.

Figure 5 shows the population changes of susceptible and infected rice plants. P_0 decreased in population early on, stabilizing at 1000 plants in the first three months because infected vector fed on them. Regardless of being P_1, P_2, and P_3 experienced an increase in population at the beginning of the first month due to P_0 being infected by vector. This shows that endemic occurs when $R_0 > 1$.

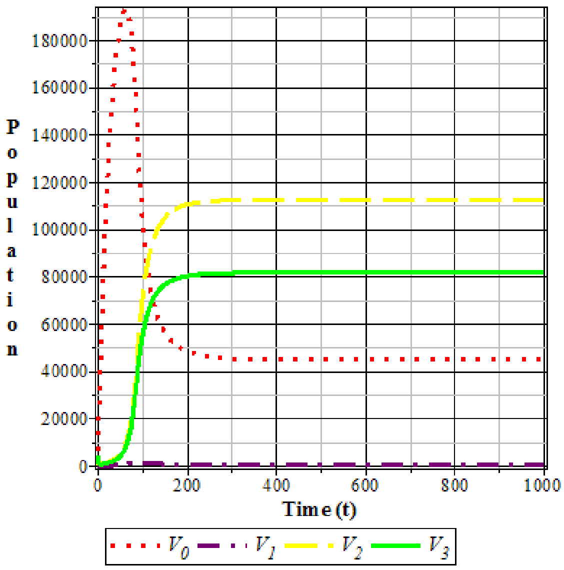

Fig. 6. Vector population dynamics when $R_0 > 1$.

Figure 6 shows the population changes of susceptible and infected vector. V_0 increased at the beginning of the first month, followed by a decrease. On the other hand, V_3 increased until it stabilized at 80,000. Meanwhile, V_2 stabilized at a higher population of more than 110,000. V_1 increased and stabilized at a population of 500. This suggests that it is endemic when $R_0 > 1$.

V. Sensitivity Analysis and Numerical Simulation

The sensitivity analysis carried out in this section consists of local sensitivity analysis and global sensitivity analysis. An example of a numerical simulation is given by varying the parameter value of λ.

A. Local Sensitivity Analysis

A sensitivity analysis of the basic reproduction number was done using a partial derivative [30]. From the results of this analysis, the sensitivity index values for case 1 and case 2 were obtained, respectively, as seen in Table II.

TABLE II
Local Sensitivity Analysis

Parameter	Sensitivity index for R_{01}	Parameter	Sensitivity index for R_{02}
B	0.50000000	B	0.500000
β	0.50000000	a	0.500000
b	0.50000000	α	0.500000
r	0.50000000	r	0.500000
q_0	-0.49999980	q_0	-0.500000
q_1	-0.49999999	q_3	-0.500000
μ	-1.00000000	μ	-0.530956
		c	-0.469043

The results in Table II, the first and second columns, show that the parameters that really influence R_{01} are the parameters $\mu, q_0, q_1, r, b, \beta,$ and B. The parameters that have a positive influence on increasing or decreasing the value of R_{01} are $\mu, q_0,$ and q_1. Meanwhile, the other four parameters negatively relate to the R_{01} value. This means that if the value of the parameters $r, b, \beta,$ and B increases, the value of R_{01} decreases.

The results in Table II, the third and fourth columns, show that the parameters influencing R_{02} are parameters $c, \mu, q_0, q_3, r, a, \alpha,$ and B. The parameters that positively influence increasing or decreasing the value of R_{02} are $c, \mu, q_0,$ and q_3. Meanwhile, the other four parameters have a negative relationship with the R_{02} value. This means that if the value of the parameters $r, a, \alpha,$ and B increases, the value of R_{02} decreases.

B. Global Sensitivity Analysis

The Latin Hypercube Sampling method and the Partial Rank Correlation Coefficient method were used for sensitivity analysis [31]. Five thousand samples were used to determine the parameters that influence the BRN, with each parameter assumed to have a value between 0 and 1. The results can be seen in Table III.

The results in Table III, the first and second columns, show that the parameters that influence R_{01} are the parameters $\mu, q_0, q_1, r, b, \beta,$ and B. The parameters that positively influence increasing or decreasing the value of R_{01} are $\mu, q_0,$ and q_1. Meanwhile, the other four parameters negatively relate to the R_{01} value. This means that if the value of the parameters $r, b, \beta,$ and B increases, the value of R_{01} decreases.

The results in Table III, the two and fourth columns, show that the parameters that influence R_{02} are parameters $c, \mu, q_0, q_3, r, a, \alpha,$ and B. The parameters that have a positive influence on increasing or decreasing the value of R_{02} are $c, \mu, q_0,$ and q_3. Meanwhile, the other four parameters negatively relate to the R_{02} value. This means that if the value of the parameters $r, a, \alpha,$ and B increases, the value R_{02} decreases.

TABLE III
Global Sensitivity Analysis Results

Parameter	Correlation Value	Parameter	Correlation Value
B	0.51526	B	0.55090
β	0.54232	a	0.57292
b	0.54200	α	0.57484
r	0.53966	r	0.57135
q_0	-0.51517	q_0	-0.54296
q_1	-0.52531	q_3	-0.55587
μ	-0.52531	μ	-0.68472
		c	-0.26881

C. Numerical Simulation

The sensitivity analysis graphs for each population are presented by providing varying λ parameter values. This is done to see the influence of these parameters on each population.

From Figure 7 to Figure 10, it can be seen that the slow parameter has little effect on P_0 and P_2. It can be seen from Figure 7 and Figure 9 that there is no significant change. Meanwhile, the parameter λ greatly influences P_1 and P_3 (shown in Figure 8 and Figure 10).

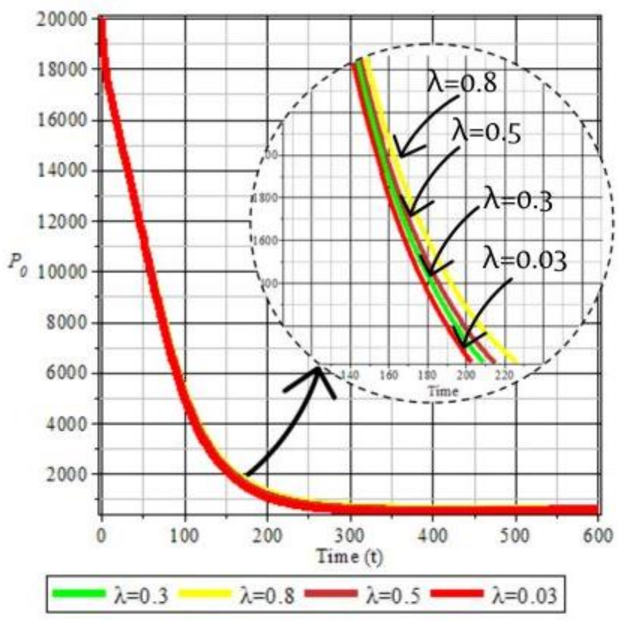

Fig. 7. Susceptible rice populations

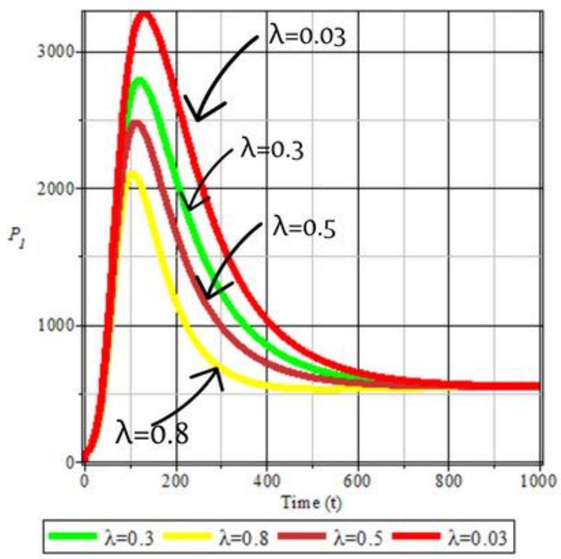

Fig. 8. Population of P_1

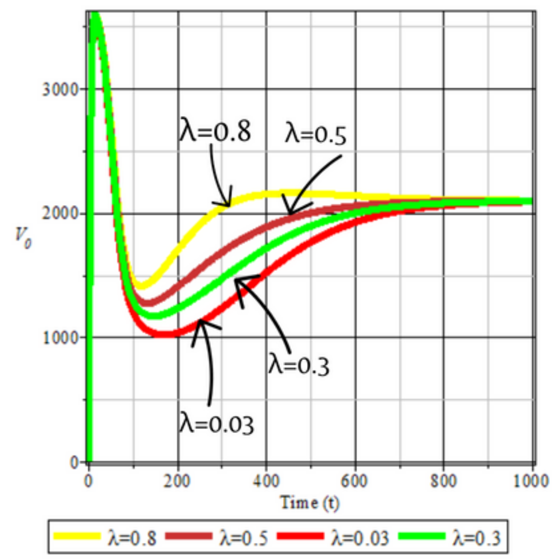

Fig. 11. Population of V_0

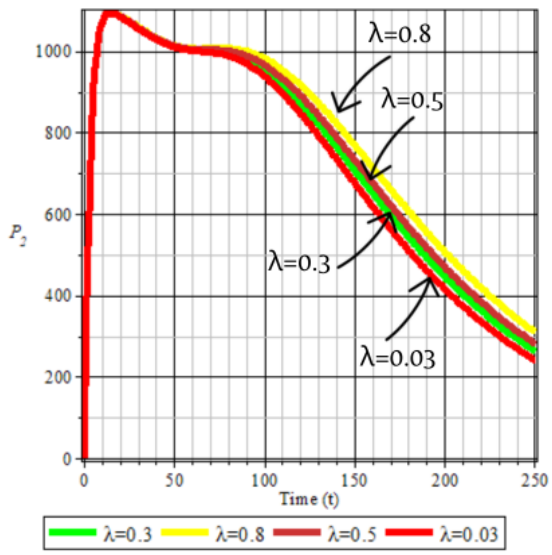

Fig. 9. Population of P_2

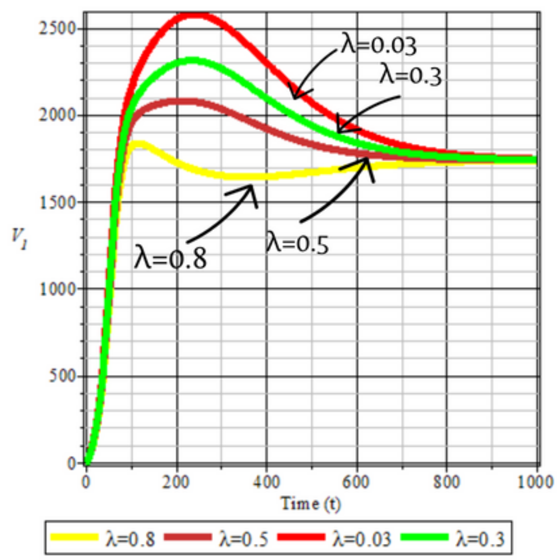

Fig. 12. Population of V_1

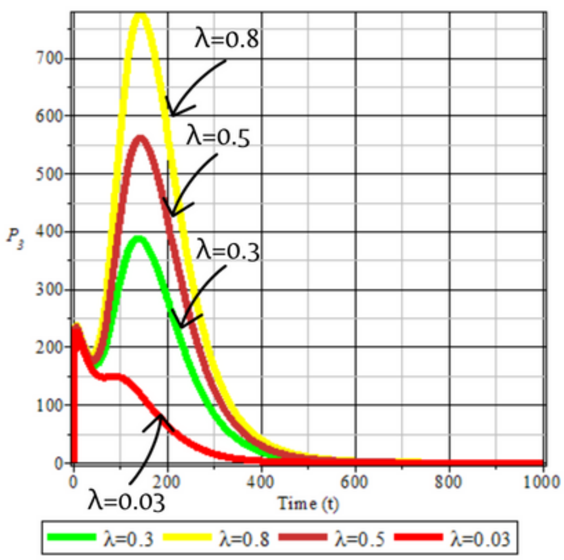

Fig. 10. Population of P_3

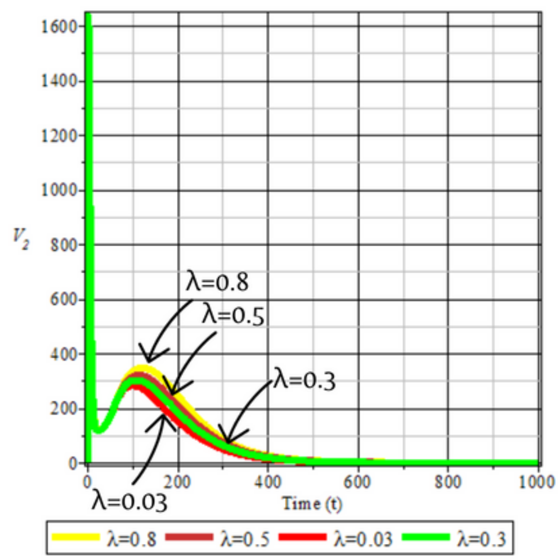

Fig. 13. Population of V_2

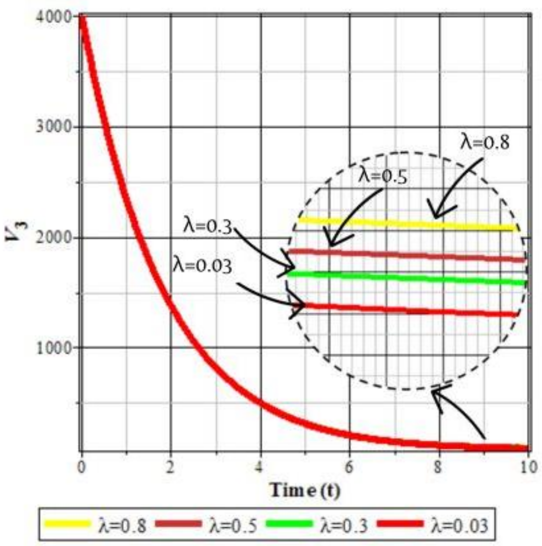

Fig. 14. Population of V_3

In contrast to rice plant populations, the λ parameter influences V_0, V_1, and V_2. This can be seen from Figure 11 to Figure 13, which shows a decrease or increase for each population when these parameters are changed. Meanwhile, V_3 had no significant effect; as seen in Figure 14, the graph shows no significant change for V_3.

VI. OPTIMAL CONTROL

A. Optimal Control Model

The optimal control model for preventing the spread of TVD minimizes the population of P_1 and P_3 by optimizing pesticide application. This is because these infected rice plants exacerbate the spread of TVD. Reducing the infected rice plant population can indirectly decrease the number of V_1 and V_3. P_2 are not treated with pesticides as they are believed to have a lower potential for spreading the TVD. The objective function used is described in equation (10).

$$J(u) = \min \int_{t_0}^{t_1} A_1P_1(t) + A_2P_3(t) + A_3V_1(t) + A_4V_3(t) + Cu^2(t)dt \tag{10}$$

$$\frac{dP_0}{dt} = r(K - N_P) - \frac{\alpha P_0V_3}{N_P} - \frac{\gamma P_0V_3}{N_P} - \frac{\tau P_0V_3}{N_P} - \frac{\beta P_0V_1}{N_P} - \frac{\sigma P_0V_2}{N_P} - q_0P_0 \tag{11}$$

$$\frac{dP_1}{dt} = \frac{\beta P_0V_1}{N_P} + \frac{\gamma P_0V_3}{N_P} - (1-u)\frac{\lambda P_1V_3}{N_P} - q_1P_1 \tag{12}$$

$$\frac{dP_2}{dt} = \frac{\tau P_0V_3}{N_P} + \frac{\sigma P_0V_2}{N_P} - \frac{\delta P_2V_3}{N_P} - q_2P_2 \tag{13}$$

$$\frac{dP_3}{dt} = \frac{\alpha P_0V_3}{N_P} + (1-u)\frac{\lambda P_1V_3}{N_P} + \frac{\delta P_2V_3}{N_P} - q_3P_3 \tag{14}$$

$$\frac{dV_0}{dt} = BN_V\left(1 - \frac{N_V}{V}\right) - \frac{uaP_3V_0}{N_P} - \frac{ubP_1V_0}{N_P} + fV_2 - \mu V_0 \tag{15}$$

$$\frac{dV_1}{dt} = \frac{ubP_1V_0}{N_P} - \frac{gP_2V_1}{N_P} - \mu V_1 \tag{16}$$

$$\frac{dV_2}{dt} = cV_3 - fV_2 - \mu V_2 \tag{17}$$

$$\frac{dV_3}{dt} = \frac{uaP_3V_0}{N_P} + \frac{gP_2V_1}{N_P} - cV_3 - \mu V_3 \tag{18}$$

With boundary conditions:
$t_0 < t < t_1, 0 \le u(t) \le 1, P_0(0) \ge 0, P_1(0) \ge 0, P_2(0) \ge 0, P_3(0) \ge 0,$
$V_0(0) \ge 0, V_1(0) \ge 0, V_2(0) > 0,$ and $V_3(0) \ge 0.$

Optimal control theory, Pontryagin's minimum principle, is used in solving the model where u is the pesticide application rate, $A_1, A_2, A_3, A_4, C \ge 0$ are the cost coefficients, and t_f is the final time. Control costs take the form of a quadratic function, where there is no linear relationship between the intervention's impact and the infected population's price [32]. Hamiltonian function is obtained as in equation (20).

$$\begin{aligned} H &= A_1P_1(t) + A_2P_3(t) + A_3V_1(t) + A_4V_3(t) + Cu^2(t) + \\ &\lambda_1\frac{dP_0}{dt} + \lambda_2\frac{dP_1}{dt} + \lambda_3\frac{dP_2}{dt} + \lambda_4\frac{dP_3}{dt} + \lambda_5\frac{dV_0}{dt} + \\ &\lambda_6\frac{dV_1}{dt} + \lambda_7\frac{dV_2}{dt} + \lambda_8\frac{dV_3}{dt} \end{aligned} \tag{19}$$

With λ_i where $i = 1, \ldots, 8$, is a costate variable often referred to as a Lagrange multiplier. According to Pontryagin's principle [33], the Hamiltonian function available in equation (21) must satisfy:
$\hat{x}(t) = [\dot{P}_0, \dot{P}_1, \dot{P}_2, \dot{P}_3, \dot{V}_0, \dot{V}_1, \dot{V}_2, \dot{V}_3]^T$,
$\hat{\lambda}(t) = [\dot{\lambda}_1, \dot{\lambda}_2, \dot{\lambda}_3, \dot{\lambda}_4, \dot{\lambda}_5, \dot{\lambda}_6, \dot{\lambda}_7, \dot{\lambda}_8]^T$, and stationary conditions.

Necessary Conditions:

$$\frac{\partial P_0}{\partial t} = \frac{\partial H}{\partial \lambda_1} = r(K - N_P) - \frac{\alpha P_0V_3}{N_P} - \frac{\gamma P_0V_3}{N_P} - \frac{\tau P_0V_3}{N_P} - \frac{\beta P_0V_1}{N_P} - \frac{\sigma P_0V_2}{N_P} - q_0P_0$$

$$\frac{\partial P_1}{\partial t} = \frac{\partial H}{\partial \lambda_2} = \frac{\beta P_0V_1}{N_P} + \frac{\gamma P_0V_3}{N_P} - (1-u)\frac{\lambda P_1V_3}{N_P} - q_1P_1$$

$$\frac{\partial P_2}{\partial t} = \frac{\partial H}{\partial \lambda_3} = \frac{\tau P_0V_3}{N_P} + \frac{\sigma P_0V_2}{N_P} - \frac{\delta P_2V_3}{N_P} - q_2P_2$$

$$\frac{\partial P_3}{\partial t} = \frac{\partial H}{\partial \lambda_4} = \frac{\alpha P_0V_3}{N_P} + (1-u)\frac{\lambda P_1V_3}{N_P} + \frac{\delta P_2V_3}{N_P} - q_3P_3$$

$$\frac{\partial V_0}{\partial t} = \frac{\partial H}{\partial \lambda_5} = BN_V\left(1 - \frac{N_V}{V}\right) - \frac{uaP_3V_0}{N_P} - \frac{ubP_1V_0}{N_P} + fV_2 - \mu V_0$$

$$\frac{\partial V_1}{\partial t} = \frac{\partial H}{\partial \lambda_6} = \frac{ubP_1V_0}{N_P} - \frac{gP_2V_1}{N_P} - \mu V_1$$

$$\frac{\partial V_2}{\partial t} = \frac{\partial H}{\partial \lambda_7} = cV_3 - fV_2 - \mu V_2$$

$$\frac{\partial V_3}{\partial t} = \frac{\partial H}{\partial \lambda_8} = \frac{uaP_3V_0}{N_P} + \frac{gP_2V_1}{N_P} - cV_3 - \mu V$$

Co-state:

$$\dot{\lambda}_1 = -\frac{\partial H}{\partial P_0} = -\lambda_1\left(-\frac{\alpha V_3}{N_P} - \frac{\gamma V_3}{N_P} - \frac{\tau V_3}{N_P} - \frac{\beta_0 V_1}{N_P} - \frac{\sigma_0 V_2}{N_P} - q_0\right) - \frac{\lambda_4\alpha_0V_3}{N_P}$$

$$\dot{\lambda}_2 = -\frac{\partial H}{\partial P_1} = -A_1 - \frac{\lambda_4(1-u)\lambda V_3}{N_P} + \frac{\lambda_5 ubV_0}{N_P}$$

$$\dot{\lambda}_3 = -\frac{\partial H}{\partial P_2} = -\frac{\lambda_4\delta V_3}{N_P} - \frac{\lambda_8 gV_1}{N_P}$$

$$\dot{\lambda}_4 = -\frac{\partial H}{\partial P_3} = -A_2 + \lambda_4q_3 + \frac{\lambda_5 aV_0}{N_P} - \frac{\lambda_8 uaV_0}{N_P}$$

$$\dot{\lambda}_5 = -\frac{\partial H}{\partial V_0} = -\lambda_5\left(-\frac{uaP_3}{N_P} - \frac{ubP_1}{N_P} - \mu\right) - \frac{\lambda_8 uaP_3}{N_P}$$

$$\dot{\lambda}_6 = -\frac{\partial H}{\partial V_1} = -A_3 + \frac{\lambda\beta V_1}{N_P} - \frac{\lambda_8 gP_2}{N_P}$$

$$\dot{\lambda}_7 = -\frac{\partial H}{\partial V_2} = \frac{\lambda_1\sigma P_0}{N_P} - \lambda_5 f + \lambda_7(f + \mu)$$

$$\dot{\lambda}_8 = -\frac{\partial H}{\partial V_3} = -A_4 - \lambda_1\left(\frac{\alpha P_0}{N_P} - \frac{\gamma P_0}{N_P} - \frac{\tau P_0}{N_P}\right) - \lambda_4\left(\frac{\alpha P_0}{N_P} + \frac{(1-u)\lambda P_1}{N_P} + \frac{\delta P_2}{N_P}\right)$$

Stationary condition:

$$u^* = \frac{\lambda_4P_1V_3\lambda + \lambda_5P_1V_0b + \lambda_5P_3V_0a - \lambda_8P_3V_0a}{2CN_P}.$$

Since $0 \le u(t) \le 1$,
then:

$$u^* = \max\left\{ \min\left[\frac{\lambda_4 P_1 V_3 \lambda + \lambda_5 P_1 V_0 b + \lambda_5 P_3 V_0 a - \lambda_8 P_3 V_0 a}{2CN_P}, 1 \right], 0 \right\}.$$

B. Effect of Pesticides

A numerical simulation of the optimal control model is presented using parameter values and variables as in Table II to see the effect of pesticides.

Figures 15 to 22 show the population dynamics of rice plants and vectors treated with pesticides on P_1 and P_3. Meanwhile, Figures 15 and 19 show that P_0 and V_0 have lower populations when not treated with pesticides. Conversely, the P_1, P_2, P_3, V_1, V_2, and V_3 decrease when pesticides are applied to P_1. This indicates that the use of pesticides on P_3 reduce P_1, P_2, P_3, V_1, V_2, and V_3.

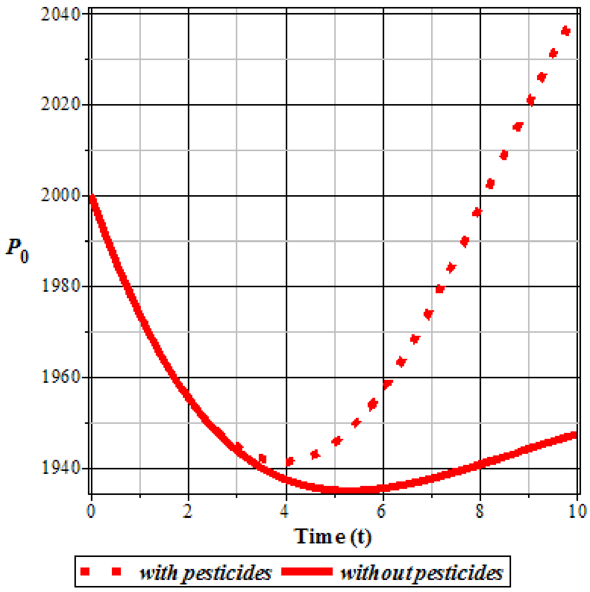

Fig. 15. Differences in P_0 with and without pesticides

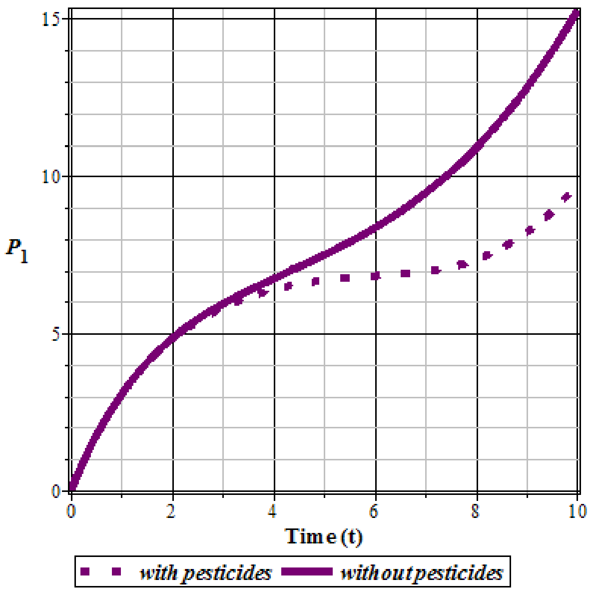

Fig. 16. Differences in P_1 with and without pesticides.

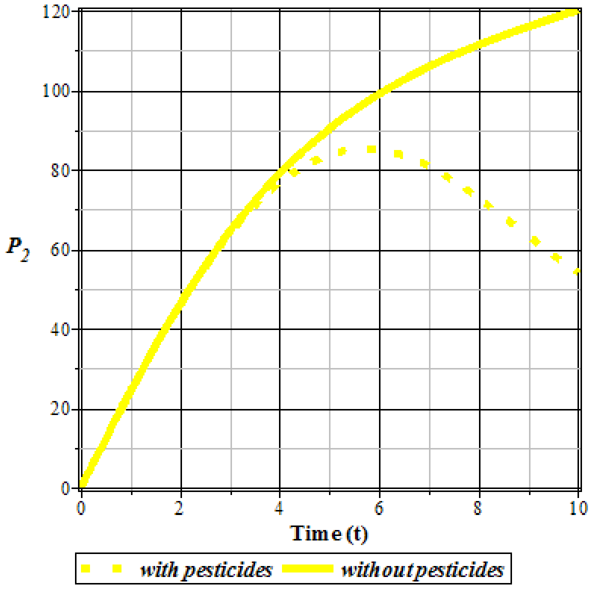

Fig. 17. Differences in P_2 with and without pesticides.

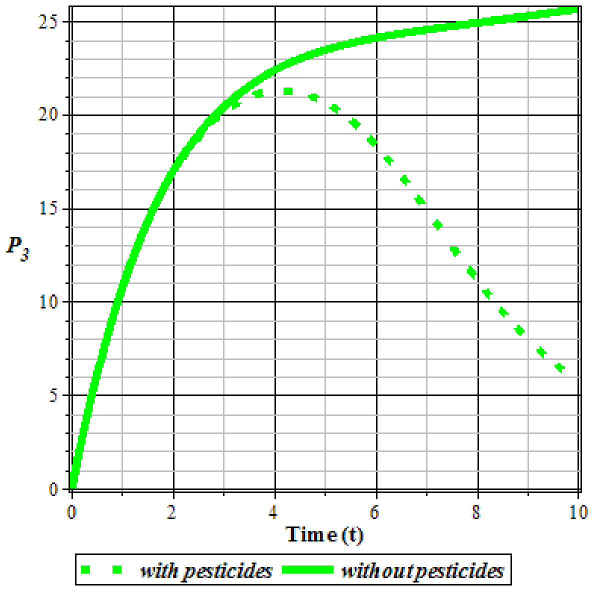

Fig. 18. Differences in P_3 with and without pesticides

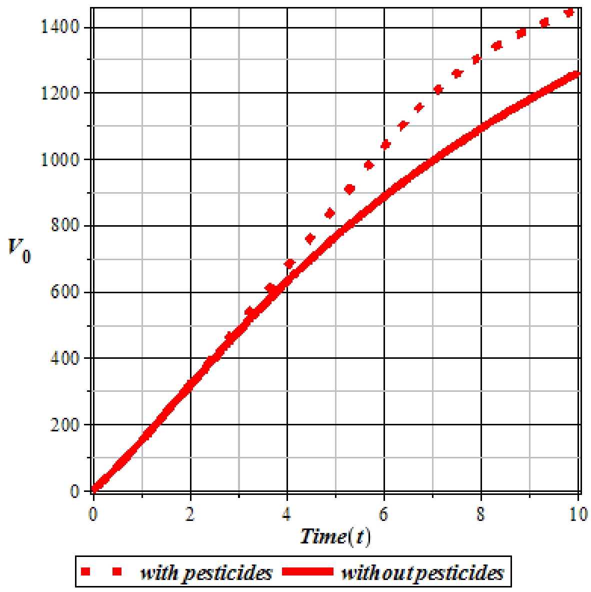

Fig. 19. Differences in V_0 with and without pesticides.

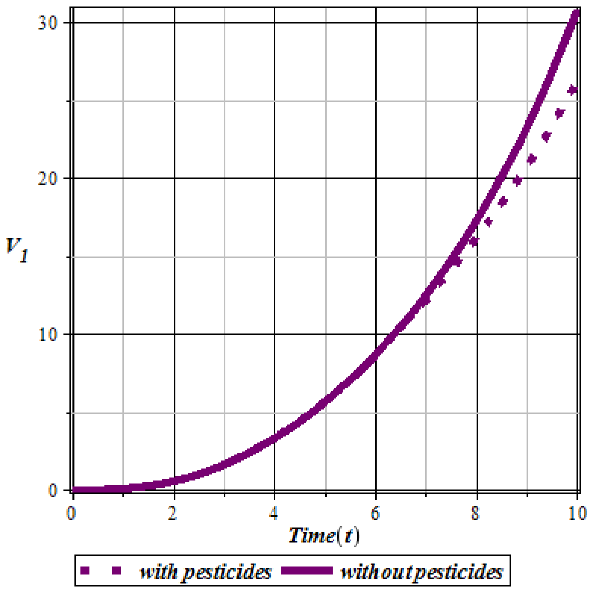

Fig. 20. Differences in V_1 with and without pesticides

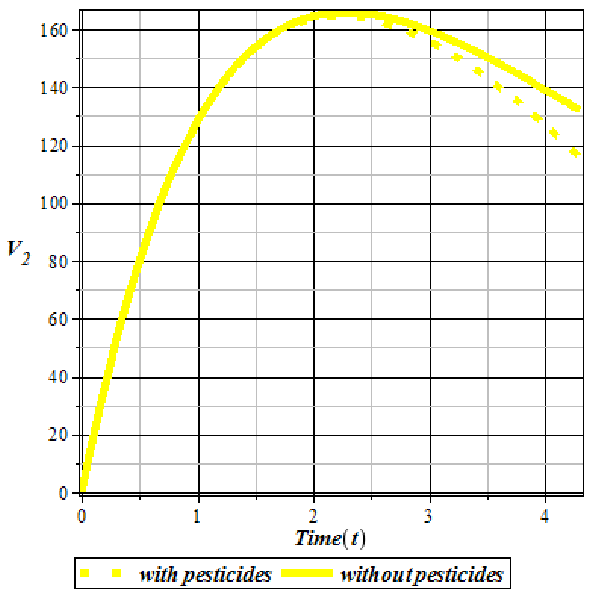

Fig. 21. Differences in V_2 with and without pesticides

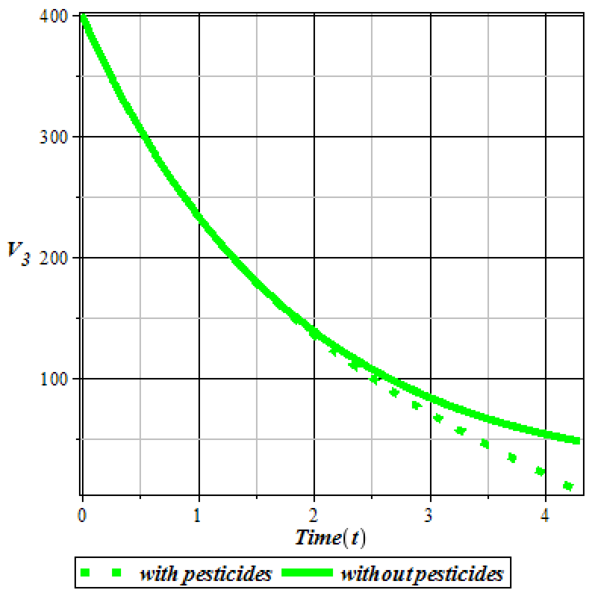

Fig. 22. Differences in V_3 with and without pesticides.

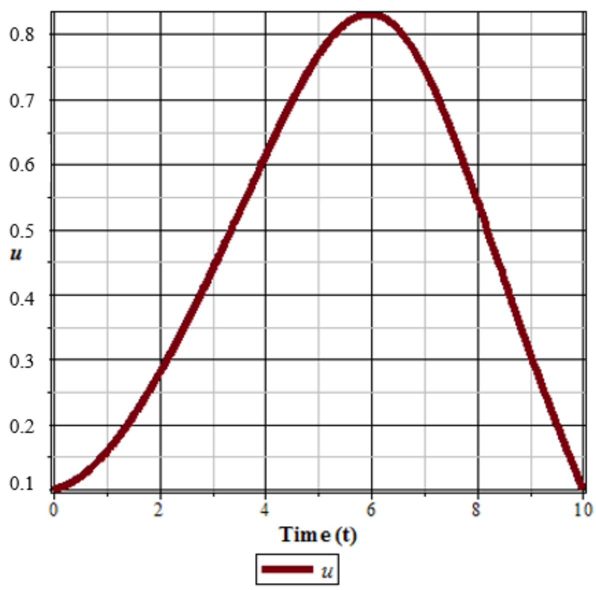

Fig. 23. Provision of pesticide control

Pesticides are administered in increments, starting from 1% of the usual dose and gradually increasing to 80%. On the sixth day, the pesticide application reaches 80%; on day seven, the application decreases until the tenth day. This dosing strategy aims to minimize costs and prevent the spread of the tungro virus disease, which could lead to financial losses for farmers and affect soil fertility and rice quality.

VII. Conclusion

The spread of TVD, taking into account the characteristics of the virus, will become endemic if $R_0 > 1$, and the DFEP will be asymptotically stable if $R_0 < 1$. In addition, optimal control results show that pesticides can control the spread of TVD. This can be seen from the optimal control model simulation results, which show that pesticide use, P_1, P_2, P_3, V_1, V_2, and V_3 decrease more rapidly than those without pesticides. The optimal use of pesticides is according to the recommended dose.

References

[1] V. Soelaiman and A. Ernawati, "Pertumbuhan dan Perkembangan Cabai Keriting (Capsicum annuum L.) secara In Vitro pada beberapa Konsentrasi BAP dan IAA," *Bul. Agrohorti* , vol. 1, no. 1, pp. 62-66, 2013.

[2] L. Sebayang, Teknik Pengendalian Penyakit Kuning pada Tanaman Cabai, Sumatra Utara: BPTP, 2013.

[3] G. N. Agrios, Plant Pathology, Fifth ed., Department of Plant Pathology University of Florida: Elsivier Academic Press, 2004.

[4] O. Azzam and T. C. B. Chancellor, "The Biology, Epidemiology, and Management of Rice Tungro Disease in Asia," *Plant Disease*, pp. 86 (2) 88-100, 2002.

[5] O. Azzam, R. C. Cabunagan and T. Chancellor, Methods for Evaluating Resistance to Rice Tungro Disease, Philippines: International Rice Resea.ch Institute, 2000.

[6] Bunawan, "Rice Tungro Disease: From Identification to Disease Control," *World Applied Sciences Journal* , vol. 31, no. 6, pp. 1221-1226, 2014.

[7] J. Shim, "Rice Tungro Spherical Virus Resistance Into Photoperiod-Insensitive Japonica Rice By Marker-Assisted Selection," *Breeding Science* , vol. 65, p. 345–351 , 2015.

[8] A. Meilin, Hama dan Penyakit pada Tanaman Cabai serta Pengendaliannya, Jambi: Balai Pengkajian Teknologi Pertanian, 2014.

[9] R. Amelia, N. Anggriani, N. Istifadah and A. K. Supriatna, "Stability Analysis for Yellow Virus Disease Mathematical Model of Red Chili Plants," *Journal of Physics: Conference Series,* vol. 1722, no. 012043, pp. 1-8, 2021.

[10] R. Amelia, N. Anggriani, N. Istifadah and A. K. Supriatna, "Dynamic Analysis of Mathematical Model of the Spread of Yellow Virus in Red Chili Plants through Insect Vectors with Logistical Functions," *AIP Conference Proceedings* , vol. 2264, no. 040006, pp. 1-10, 2020.

[11] R. Amelia, M. Mardiyah, J. Nahar, N. Anggriani and A. K. Supriatna, "Optimal Control for The Use Of Botanical Fungicides in The Spread of Plant Diseases," *IOP Conf. Series: Journal of Physics: Conf. Series,* pp. 1315 (2019) 012054 doi:10.1088/1742-6596/1315/1/012054, 2019.

[12] R. Amelia, N. Anggriani and A. K. Supriatna, "Optimal Control Model of *Verticillium lecanii* Application in the Spread of Yellow Red Chili Virus," *WSEAS Transactions on Mathematics,* pp. 351-358, 2019.

[13] N. Anggriani, N. Istifadah, M. Hanifah and A. K. Supriatna, "A Mathematical Model of Protectant and Curative Fungicide Application and its Stability Analysis," *IOP Conf. Series: Earth and Environmental Science,* p. 31, 2016.

[14] N. Anggriani, D. Arumi, E. Hertini, N. Istifadah and A. K. Supriatna, "Dynamical Analysis of Plant Disease Model with Roguing, Replanting and Preventive Treatment," *Proceedings of 4th International Conferenve on Research, Implementation, and Education of Mathematics and Science,* 2017.

[15] N. Anggriani, M. Ndii, D. Arumi, N. Istifadah and A. K. Supriatna, "Mathematical Model for Plant Disease Dynamics With Curative and Preventive Treatment," *Journal of Physics: Conf. Series,* 2018.

[16] N. Anggriani, R. Amelia, N. Istifadah and D. Arumi, "Optimal Control of Plant Disease Model with Roguing, Replanting, Curative, and Preventive Treatment," *Journal of Physics: Conference Series,* vol. 1657, no. 012050, pp. 1-6, 2020.

[17] N. Anggriani, L. N. Putri and A. K. Supriatna, "Stability Analysis and Optimal Control Plant Fungal: an Explicit Model with Curative Factor," *AIP Conference Proceedings,* pp. 1651, 40, 2015.

[18] N. Anggriani, M. Yusuf and A. K. Supriatna, "The Effect of Insecticide on The Vector of Rice Tungro Disease: Insight From A Mathematical Model," *International Interdisciplinary Journal,* pp. 20, 9A, 2017.

[19] N. Anggriani, M. Z. Ndii, N. Istifadah and A. K. Supriatna, "Disease Dynamics with Curative and Preventive Treatments in a Two-Stage Plant Disease Model," in *The 6th International Conference on Science & Engineering in Mathematics, Chemistry and Physics AIP Conf,* 2018.

[20] N. Anggriani, M. Mardiyah, N. Istifadah and A. K. Supriatna, "Optimal Control Issues in Plant Disease with Host Demographic Factor and Botanical Fungicides," *IOP Conference Series: Materials Science and Engineering,* pp. 1-11, 2018.

[21] D. Arumi, N. Anggriani and E. Hertini, "Disease Dynamics with Curative and Preventive Treatments in A Two-Stage Plant Disease Model," in *Prosiding Seminar Nasional ke-2: Sains, Rekayasa & Teknologi UPH*, 2017.

[22] D. A. Putri, N. Anggriani and E. Hertini, "Analisis Dinamik Model Penyakit Tanaman Kakao melalui Roguing dan Replanting dengan Faktor Treatment Curative," in *Seminar Nasional ke-2: Sains, Rekayasa & Teknologi UPH - 2017* , Tangerang, 2017.

[23] W. Suryaningrat, N. Anggriani, A. K. Supriatna and N. Istifadah, "The Optimal Control of Rice Tungro Disease with Insecticide and Biological Agent," *AIP Conference Proceedings,* vol. 2264, pp. 1-12, 2020.

[24] A. Maryati, N. Anggriani and E. Carnia, "Stability Analysis of Tungro Disease Spread Model in Rice Plant Using Matrix Method," *Barekeng,* vol. 16, no. 1, pp. 217-228, 2022.

[25] W. Suryaningrat, N. Anggriani and A. K. Supriatna, "Mathematical Analysis and Numerical Simulation of Spatial-Temporal Model for Rice Tungro Disease Spread," *Communications in Mathematical Biology and Neuroscience,* pp. 1-13, 2022.

[26] N. T. Blas, J. M. Addawe and G. David, "A Mathematical Model of Transmission of Rice Tungro Disease by *Nephotettix virescens*," *The American Institute of Physics,* vol. 1787, no. 080015, pp. 080015-1–080015-7, 2016.

[27] N. Blas and G. David , "Dynamical Roguing Model for Controlling The Spread of Tungro Virus Via *Nephotettix virescens* in A Rice Field," *Journal of Physics: Conf. Series,* p. 893 (012018), 2017.

[28] R. Amelia, N. Anggriani, A. K. Supriatna and N. Istifadah, "Mathematical Model for Analyzing the Dynamics of Tungro Virus Disease in Rice: A Systematic Literature Review," *Mathematics MDPI,* vol. 10, no. 2944\, pp. 1-18, 2022.

[29] P. van den Driessche and J. Watmough, "Reproduction Numbers and Sub-Threshold Endemic Equilibria for Compartmental Models of Disease Transmission," *Mathematical Biosciences,* vol. 180, no. 1-2, pp. 29-48, 2002.

[30] N. Chitnis, J. M. Hyman and J. M. Cushing, “Determining Important Parameters in The Spread of Malaria Through The Sensitivity Analysis of A Mathematical Model,” *Bulletin of Mathematical Biology,* vol. 70, pp. 1272–1296, 2008.

[31] S. Marino, I. B. Hogue, C. J. Rayand D. E. Kirschner, “A Methodology for Performing Global Uncertainty and Sensitivity Analysis in Systems Biology,” *Journal of theoretical biology,* 254(1), pp. 178-196, 2008.

[32] F. Agusto and . M. Khan, "Optimal Control Strategies for Dengue Transmission in Pakistan," *Mathematical Biosciences,* p. doi: https://doi.org/10.1016/j.mbs.2018.09.007, 2018.

[33] S. Lenhart and J. T. Workman, Optimal Control Applied to Biological Models, CRC Press, taylor & Francis Group, 2007.